

# A new approach to measure melamine, cyanuric acid, and melamine cyanurate using surface enhanced Raman spectroscopy coupled with gold nanosubstrates

Lili He · Yang Liu · Mengshi Lin · Joseph Awika · David R. Ledoux · Hao Li · Azlin Mustapha

Received: 16 November 2007 / Accepted: 30 January 2008 / Published online: 1 March 2008  
© Springer Science+Business Media, LLC 2008

**Abstract** Vibrational spectroscopic characteristics of melamine, cyanuric acid, and melamine cyanurate were measured using surface-enhanced Raman spectroscopy (SERS) coupled with gold nanosubstrates. Trace amounts of melamine and its analogues (cyanuric acid and melamine cyanurate) were characterized and quantified quickly and accurately by SERS in combination with partial least squares (PLS) analysis. Based on the relationship between the Raman intensity of the most prominent peak at around  $676\text{ cm}^{-1}$  and log values of melamine concentrations, the limit of detection (LOD) of SERS for melamine was estimated to be  $2.6 \times 10^{-7}\text{ mol L}^{-1}$  ( $\sim 33\text{ ppb}$ ). An approximately  $3 \times 10^4$  fold of enhancement factor for SERS signals of melamine on gold nanosubstrates was obtained. This result was based upon the comparison of the peak at around  $676\text{ cm}^{-1}$  in the SERS spectra with that of normal Raman spectra of melamine in aqueous solutions. SERS spectra of cyanuric acid acquired from its solid form differ significantly from this compound in an aqueous solution, indicating a possible keto-enol isomerization reaction of cyanuric acid in water. When equal amounts of melamine and cyanuric acid were added together, spoke-like crystals of melamine cyanurate formed instantly,

which could be measured and characterized by SERS. This study demonstrates that SERS could provide a fast and ultra-sensitive tool for detection and characterization of melamine and its derivative compounds in aqueous solutions.

**Keywords** Melamine · Cyanuric acid · Melamine cyanurate · SERS · Gold nanosubstrate

## Introduction

Since early 2007, there has been mounting concern about the intentional adulteration of protein ingredients used in pet foods and human foods with melamine. By November 2007, 244 cases of pet deaths and 348 cases of kidney disease in pets had been confirmed in the United States, prompting massive recalls of pet foods, livestock feeds and feeds used in commercial aquaculture and hatcheries, particularly in the United States and Canada [1]. The economic impact on the pet food market and the industry has been enormous.

Melamine (2,4,6-triamino-1,3,5-triazine), along with its derivative compounds (e.g. cyanuric acid, melamine cyanurate, etc), were implicated in this pet food contamination. Melamine is often combined with formaldehyde to produce melamine resin, a heat tolerant polymer commonly used in kitchenware, fire retardant fabrics, and commercial filters [2]. It is believed that melamine or cyanuric acid was intentionally added into food ingredients to make the products appear to contain a higher protein content than they actually did due to high nitrogen content of melamine and cyanuric acid.

However, neither melamine nor cyanuric acid is thought to be highly toxic to humans. A current hypothesis

L. He · Y. Liu · M. Lin (✉) · J. Awika · A. Mustapha  
Food Science Program, Division of Food Systems &  
Bioengineering, University of Missouri, Columbia,  
MO 65211, USA  
e-mail: linme@missouri.edu

D. R. Ledoux  
Department of Animal Sciences, University of Missouri,  
Columbia, MO 65211, USA

H. Li  
Department of Mechanical and Aerospace Engineering,  
University of Missouri, Columbia, MO 65211, USA

is that the toxicity increases when melamine and cyanuric acid are present together [3]. Melamine and cyanuric acid can form a hydrogen-bonded bimolecular network by a surface-based self-assembly process [4]. “Spoke-like” crystals have been found in contaminated wheat gluten and rice protein concentrate imported from overseas, as well as in the tissues and urine of affected animals. The extremely insoluble crystals formed in animal kidneys were suspected of compromising kidney function, leading to acute renal failure in cats and dogs. These crystals, serving as a biomarker for contamination, contain melamine, cyanuric acid, melamine cyanurate, and other related compounds [5].

In April 2007, the US Food and Drug Administration (FDA) and the U.S. Department of Agriculture (USDA) acknowledged that thousands of hogs and chickens that were fed tainted animal feed had been processed into human foods. Although government scientists concluded that there is a very low risk of melamine to human health from consuming foods made from animals that ate the tainted feed [6], melamine is not a substance that should be present in foods at any level. Trace amounts of melamine in foodstuff have been previously reported due to migration from melamine-containing resins [2, 7] and the presence of the metabolic product of cyromazine which is an insecticide used on crops [8]. Until the 2007 pet food recalls, melamine in foodstuffs was not routinely monitored since there was no reason to expect that a supplier would intentionally commit this type of economic fraud.

Recently, great advances have been made in the development of a novel and ultra-sensitive vibrational spectroscopic method—surface-enhanced Raman spectroscopy (SERS). SERS has a great potential for detecting samples on a nanosubstrate with a limit of detection (LOD) down to the parts-per-billion (ppb) level or even a single molecule [9]. SERS is a branch of Raman spectroscopy that measures molecular vibrations by light scattering. During the measurement, the incident laser light is inelastically scattered from a sample and the frequency or wavelength of this light shifts in a manner of characteristic molecular vibrations [10, 11]. However, signals of conventional Raman spectroscopy are very weak because only one photon in one million will scatter inelastically (Raman shift). When probed molecules attach to metallic nanostructures (typically, Au, Ag, Cu, Pt or Pd), Raman signals can be significantly enhanced by millions of times in high localized optical fields of these structures due to “electromagnetic field enhancement” and “chemical or electronic enhancement” of signals [12, 13]. Furthermore, SERS is capable of measuring samples non-destructively, on-line, in real-time, and with minimum interference from water.

The objectives of this study were to characterize vibrational spectroscopic properties of melamine, cyanuric

acid, and melamine cyanurate, and to investigate the feasibility of using SERS coupled with novel gold nanosubstrates to measure trace amounts of melamine and other related compounds in an aqueous solution.

## Materials and methods

### Preparation of chemical samples

Melamine and cyanuric acid were purchased from Fisher Scientific Inc. (Pittsburgh, PA, USA). Both melamine and cyanuric acid are poorly soluble in water with a solubility of about  $2.5 \times 10^{-2}$  for melamine and  $2.0 \times 10^{-2}$  mol L<sup>-1</sup> for cyanuric acid at 25°C [14]. In this study, a series of concentrations ( $10^{-2}$ ,  $10^{-3}$ ,  $10^{-4}$ ,  $10^{-5}$ ,  $10^{-6}$ , and  $10^{-7}$  mol L<sup>-1</sup>) of melamine in water were prepared. An aqueous solution of cyanuric acid ( $10^{-3}$  mol L<sup>-1</sup>) was also prepared by dissolving in water with stirring; when cyanuric acid particles were completely dissolved, the solution was analyzed immediately by SERS. Melamine cyanurate was prepared by adding equal amounts ( $10^{-3}$  mol L<sup>-1</sup>) of melamine and cyanuric acid together in a glass container.

### SERS instrumentation

A Renishaw RM1000 Raman Spectrometer System (Gloucestershire, UK) equipped with a Leica DMLB microscope (Wetzlar, Germany) was used in this study. This system is equipped with a 785 nm near-infrared diode laser source. During the measurement, light from the high power (maximum at 300 mW) diode laser was directed and focused onto the sample on a microscope stage through a 50× objective. A color video camera (Sony Inc, Towada, Japan) was attached to the microscope. Raman scattering signals were detected by a 578 × 385 pixels CCD array detector. The size of each pixel was 22 μm × 22 μm. Spectral data were collected by the WiRE 1.3 software (Gloucestershire, UK).

### Gold nanosubstrates

Klarite™ SERS-active substrates (D3technologies Ltd, Hampshire, UK) were used. These devices were fabricated on silicon wafers coated with gold. A 6 mm × 10 mm chip including a 4 mm × 4 mm patterned SERS-active area and an unpatterned gold reference area was adhered to a standard 25 mm × 75 mm microscope slide. Nanotextured pyramidal subunits begin as ~1.8 μm openings, which are monotonically tapered over ~1.0 μm deep depression and arranged in a square lattice configuration at a separation of ~0.4 μm.

## Data analysis

SERS spectral data were analyzed by Delight version 3.2.1 (D-Squared Development Inc., LaGrande, OR, USA) software. Pre-processing algorithms were employed to analyze the data, such as polynomial subtract and smoothing. Effects such as light scattering and detector response that have a wavelength dependency could be corrected by Polynomial subtract. Smoothing eliminates high-frequency instrumental noises by averaging neighboring data points. In this study, spectra of samples were collected using a 50 $\times$  objective with a detection range from 300 to 1800  $\text{cm}^{-1}$  in the extended mode. The measurement was conducted with a 10 s exposure time and  $\sim 20$  mW laser power. SERS spectra data were first applied with the third polynomial subtract and smoothed with a Gaussian function over 8  $\text{cm}^{-1}$ . Prior to partial least squares (PLS) analysis, spectral samples were preprocessed using Savistky–Golay second derivative transformation (10  $\text{cm}^{-1}$ ) to offset baseline shift. Correlations between spectral features and actual values were used to predict melamine concentration in tested samples. PLS model was validated by leave-one-out cross validation, which uses all but one sample to build a calibration model and repeats for each sample in the data set [15, 16]. The performance of the model was indicated by  $R^2$  (predicted against actual values) and the root mean square error of prediction

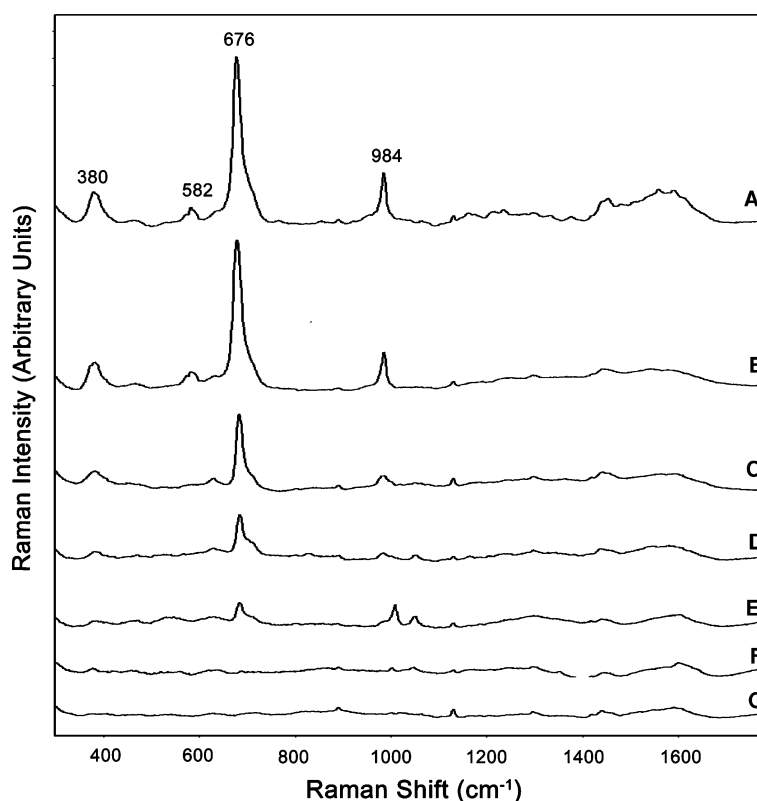
(RMSEP). A higher  $R^2$  and a lower RMSEP indicate a better model. The number of PLS latent variables was optimized based on the lowest RMSEP values to avoid over fitting of spectral data [16].

## Results and discussion

The average spectra ( $n = 4$ ) of different concentrations of melamine solution are shown in Fig. 1. Typical Raman peaks at 380, 582, 676, 984  $\text{cm}^{-1}$  were observed. The most intense peak at 676  $\text{cm}^{-1}$  is assigned to the ring breathing II mode and involves in-plane deformation of the triazine ring. The second highest peak at 984  $\text{cm}^{-1}$  arises from the ring breathing mode I of the triazine ring [17]. No peaks were observable in the SERS spectra obtained from the melamine sample with a concentration of  $10^{-7}$  mol  $\text{L}^{-1}$  or lower.

For the PLS analysis, the best performance was achieved using the full spectral region (300–1800  $\text{cm}^{-1}$ ) with four latent variables. Figure 2 shows the RMSEP of melamine PLS models with different latent variables. The lowest RMSEP was found when four latent variables were used, indicating that the optimal number of latent variable is four. Figure 3 shows the PLS prediction results by constructing the log values of predicted melamine concentrations against the log values of actual melamine

**Fig. 1** SERS spectra (300 to 1800  $\text{cm}^{-1}$ ) of different concentrations of melamine:  $10^{-2}$  (a),  $10^{-3}$  (b),  $10^{-4}$  (c),  $10^{-5}$  (d),  $10^{-6}$  (e), and  $10^{-7}$  (f) mol  $\text{L}^{-1}$ ; (g) gold substrate without the sample. Measurement was conducted with a 10 s exposure time and  $\sim 20$  mW laser power



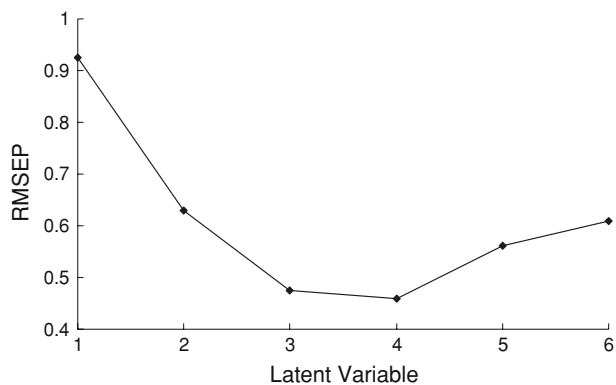


**Fig. 2** Root mean square error of prediction (RMSEP) values of the partial least squares (PLS) models for melamine with different latent variables

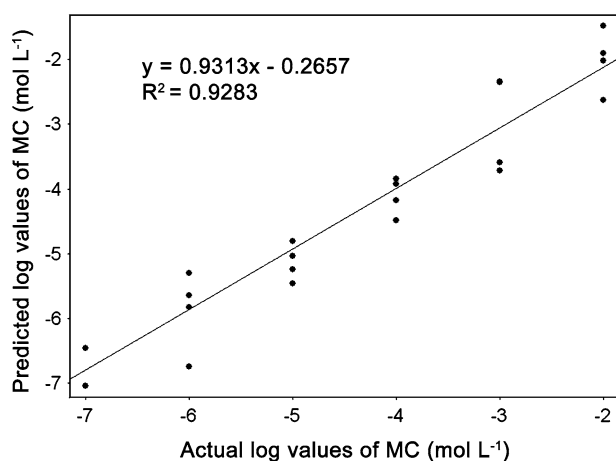


**Fig. 3** Partial least squares (PLS) prediction model of log values of melamine concentration (MC) ( $\text{mol L}^{-1}$ )

concentrations. A good prediction result was obtained ( $R^2 = 0.93$ ,  $\text{RMSEP} = 0.46$ ).

Another prediction model was constructed based on the relationship between the intensity of the highest peak in melamine SERS spectra at around  $676 \text{ cm}^{-1}$  and log values of melamine concentrations. Theoretically, higher concentrations of test samples should result in a stronger Raman intensity. However, in reality, increasing the sample concentration over a certain level will saturate the detector. A linear regression ( $R^2 = 0.96$ ) was found between Raman intensity and melamine concentrations (Fig. 4). Therefore, based upon the results calculated by linear regression, the LOD for melamine using this SERS method is  $2.6 \times 10^{-7} \text{ mol L}^{-1}$ , which is equivalent to approximately 33 ppb. This special model is reasonable for melamine because only one prominent featured peak was present in the melamine SERS spectra. Although it is only based on one peak, this model is applicable when applied in different complex systems since it excludes other

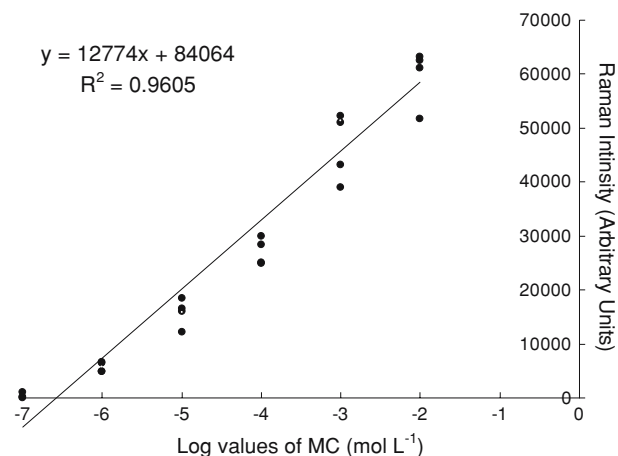


**Fig. 4** Relationship between Raman intensity of the highest peak at around  $676 \text{ cm}^{-1}$  and log value of melamine concentration (MC)

interferences from the systems. Additionally, it is easier and faster to establish this model than the previous one when qualitative and partial quantitative screening of melamine is desired.

To determine the enhancement factor of Klarite<sup>TM</sup> gold nanosubstrates for melamine,  $10^{-2}$  and  $10^{-4} \text{ mol L}^{-1}$  of melamine solutions were deposited onto the non-active surface and active surface of the nanosubstrate, respectively. Based on the highest peak at around  $676 \text{ cm}^{-1}$ , an approximately  $3 \times 10^4$  fold of signal enhancement in the SERS spectra of melamine over the normal spectra was calculated (Fig. 5). Additionally, a  $\sim 5 \text{ cm}^{-1}$  shift was found between these two peaks in Fig. 5a and b, probably due to different concentrations and/or the influence from the nanosubstrate. The LOD of this SERS method could potentially be even lower if better performing nanosubstrates with a higher SERS enhancement factor were used.

SERS spectra of the solid and aqueous forms of cyanuric acid ( $10^{-3} \text{ mol L}^{-1}$ ) are shown in Fig. 6. For cyanuric acid

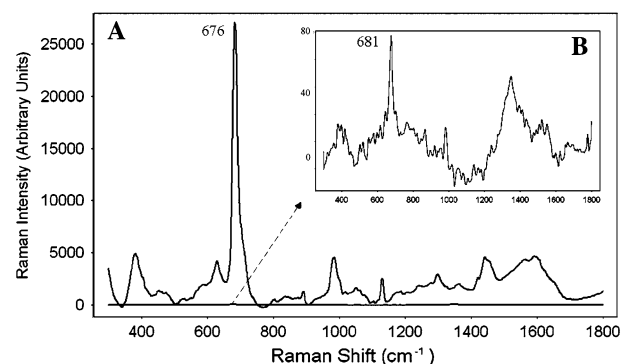


**Fig. 5** Raman spectrum of  $10^{-4} \text{ mol L}^{-1}$  melamine (a) on SERS-active area of gold nanosubstrate and  $10^{-2} \text{ mol L}^{-1}$  melamine (b) on non-active area of gold nanosubstrate. Measurement was conducted from  $300$  to  $1800 \text{ cm}^{-1}$  with a  $10 \text{ s}$  exposure time and  $\sim 20 \text{ mW}$  laser power

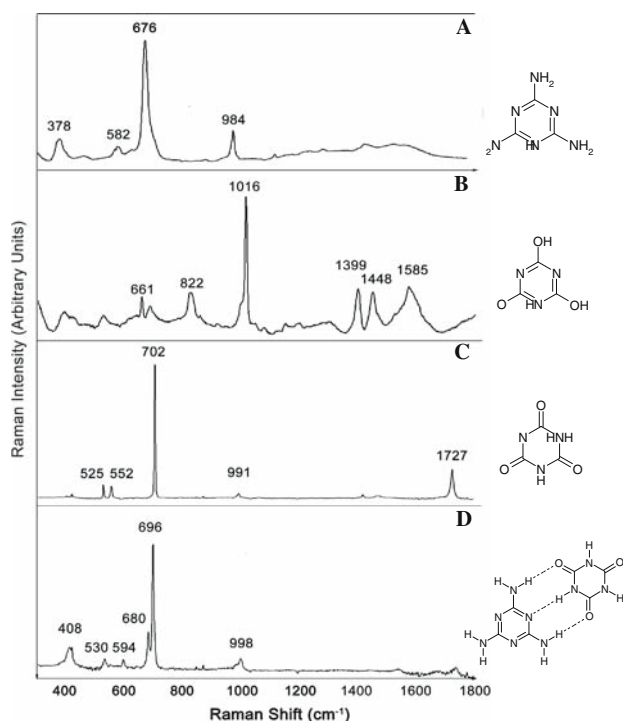


**Fig. 6** SERS spectra of  $10^{-3}$  mol  $L^{-1}$  melamine (a),  $10^{-3}$  mol  $L^{-1}$  cyanuric acid (b), solid cyanuric acid (c), melamine cyanurate (d) made from adding equal amounts ( $10^{-3}$  mol  $L^{-1}$ ) of melamine and cyanuric acid. Measurement was conducted from 300 to  $1800\text{ cm}^{-1}$  with a 10 s exposure time and  $\sim 20$  mW laser power

in the solid forms, prominent peaks were found at 525, 552, 702, 991, and  $1727\text{ cm}^{-1}$  (Fig. 6c). However, when measuring SERS spectra of the aqueous form of cyanuric acid immediately after the chemicals dissolved completely in water, prominent peaks were found at 661, 822, 1016, 1399, 1448, and  $1585\text{ cm}^{-1}$  (Fig. 6b). Some of those bands have been assigned before, such as  $702\text{ cm}^{-1}$  to a ring out-of-plane bending vibration,  $1016\text{ cm}^{-1}$  to the ring breathing, and  $1727\text{ cm}^{-1}$  to the C=O stretching [18, 19]. Interestingly, in less than one hour, small crystals were found in the cyanuric acid solution under a  $50\times$  objective; and the SERS spectrum of the solution changed back to that of the solid form. This may be due to the enol (cyanuric acid)–keto (isocyanuric acid) tautomerism.

Free cyanuric acid in crystal forms and in neutral and acid solutions exists mainly as the keto form, while in alkali solutions, the enol form is predominant [14]. Raman spectra of the keto form as a solid and in acid solutions and the enol form in alkali solution have been previously reported [18, 20]. However, in alkali solutions the compound is not present in the enol form but as a salt produced by the reaction between the enol form of cyanuric acid with the alkali. From a thermodynamics point of view, the keto-enol isomerization reaction is endothermic, indicating that the keto form is more stable than the enol form without the

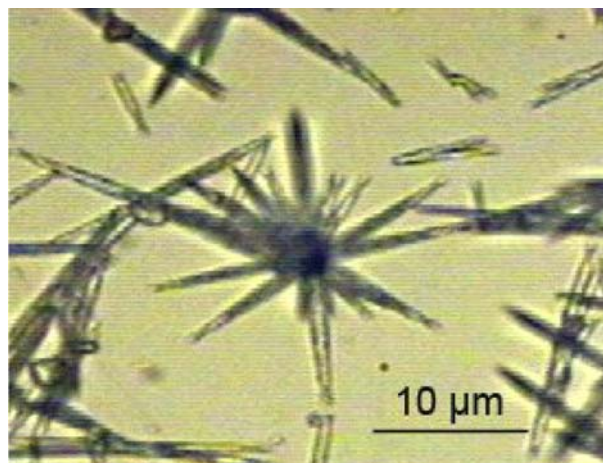


**Fig. 7** Spoke-like crystals were observed in the melamine cyanurate solution when equal amounts ( $10^{-3}$  mol  $L^{-1}$ ) of melamine and cyanuric acid were added

consideration of solvent effects [21]. While in an aqueous solution, water molecules produce an important catalytic effect, reducing the enthalpy and energy barrier of the reaction considerably, thus the reaction rates increase significantly and the keto-enol tautomerism occurs easier [22]. Therefore, it is possible that immediately after cyanuric acid dissolved in water, the SERS spectrum obtained was from the enol form of cyanuric acid due to increased energy input from the stirring; while after the stirring stopped, the unstable enol form gradually changed back to a more stable keto form.

When adding equal amounts ( $10^{-3}$  mol  $L^{-1}$ ) of melamine and cyanuric acid together, white precipitates (melamine cyanurate) instantly formed. These spoke-like crystals were clearly observed under the  $50\times$  microscope objective and captured by a color video camera (Fig. 7). The spectrum of melamine cyanurate crystals is shown in Fig. 6d. Typical peaks at 408, 530, 594, 680, 696, and  $998\text{ cm}^{-1}$  were readily observed. A similar spectrum of melamine cyanurate was obtained by Tseng et al using FT-Raman [23].

## Conclusions

SERS could provide an ultrasensitive and fast approach to measure and characterize melamine, cyanuric acid, and melamine cyanurate. With the aid of gold nanosubstrates, an approximately  $10^4$ -fold of enhancement factor was achieved in the measurement of melamine on SERS-active surfaces of gold nanosubstrates. A PLS model was built for predicting melamine concentrations. The LOD of SERS can reach the level of  $2.6 \times 10^{-7}$  mol  $L^{-1}$  ( $\sim 33$  ppb) based on the calculations of the highest peak in melamine SERS spectra at around  $676\text{ cm}^{-1}$ . Cyanuric acid and

spoke-like crystals of melamine cyanurate were also measured and characterized by SERS. As the first step to detect melamine and its analogues in food products, this preliminary study demonstrates that SERS is capable of measuring trace amounts of melamine and its related compounds in aqueous solutions, indicating its potential applications in monitoring quality and safety attributes of food samples. Currently, further studies are being conducted in our lab to detect melamine and other related compounds in real food systems.

**Acknowledgement** Special thanks are given to Dr. Barbara Rasco (Ph.D., JD) in the Department of Food Science at Washington State University for her kind review of this study.

## References

1. MSNBC. Tainted food killed 224 pets in latest tally. <http://www.msnbc.msn.com/id/22028878/from/ET/> (2007)
2. T. Sugita, H. Ishiwata, K. Yoshihira, *Food Addit. Contam.* **7**, 21 (1990)
3. C.A. Brown, K.S. Jeong, R.H. Poppenga et al., *J. Vet. Diagn. Invest.* **19**, 525 (2007)
4. L.M.A. Perdigao, N.R. Champness, P.H. Beton, *Chem. Commun.* 538 (2006)
5. W. Yi, W. Bei, Q.G. Wang, *J. Crystallogr. Spectrosc. Res.* **20**, 79 (1990)
6. M. Hostetler. Melamine risk assessment. <http://www.preparedfoods.com> (2007), p. 37
7. T. Sugita, H. Ishiwata, K. Yoshihira, A. Maekawa, *Bull. Environ. Contam. Toxicol.* **44**, 567 (1990)
8. J.V. Sancho, M. Ibanez, S. Grimalt, O.J. Pozo, F. Hernandez, *Anal Chim Acta* **530**, 237 (2005)
9. K. Kneipp, H. Kneipp, I. Itzkan, R.R. Dasari, M.S. Feld, *J. Phys. Condens. Matter.* **14**, R597 (2002)
10. K. Kneipp, H. Kneipp, I. Itzkan, R.R. Dasari, M.S. Feld, *Chem. Rev.* **99**, 2957 (1999)
11. E.B. Hanlon, R. Manoharan, T.W. Koo et al., *Phys. Med. Biol.* **45**, R1 (2000)
12. K. Kneipp, A.S. Haka, H. Kneipp et al., *Appl. Spectrosc.* **56**, 150 (2002)
13. C.L. Haynes, A.D. McFarland, R.P. Van Duyne, *Anal. Chem.* **77**, 338a (2005)
14. G.B. Seifer, *Russ. J. Coord. Chem.* **28**, 301 (2002)
15. H. Martens, T. Naes, *Multivariate Calibration* (John Wiley & Sons, Inc., New York, 1986)
16. M. Lin, A.G. Cavinato, Y. Huang, B.A. Rasco, *Food Res. Int.* **36**, 761 (2003)
17. E. Koglin, B.J. Kip, R.J. Meier, *J. Phys. Chem.* **100**, 5078 (1996)
18. D.M. Lewis, *Adv. Colour Sci. Technol.* **4**, 59 (2001)
19. M.K. Marchewka, *Mater. Lett.* **58**, 843 (2004)
20. M. Ito, *Bull. Chem. Soc. Jpn.* **26**, 339 (1953)
21. X.Q. Liang, W.X. Zheng, N.B. Wong, J.S. Li, A.M. Tian, *J. Mol. Struct-Theochem.* **672**, 151 (2004)
22. X.Q. Liang, X.M. Pu, H.W. Zhou, N.B. Wong, A.N. Tian, *J. Mol. Struct-Theochem.* **816**, 125 (2007)
23. C.H. Tseng, C.K. Mann, T.J. Vickers, *Appl. Spectrosc.* **48**, 535 (1994)